RESEARCH ARTICLE

Hydro-Geochemical Assessment of Groundwater Quality Of Muda River Basin, Kedah Malaysia

Muhammad Noor Amin Zakariah[a,b*], Norsyafina Roslan[b], Norasiah Sulaiman[b], Muhammad Amzar Bin Aznan[c]. Bilal Al Farishi[d]

[a]Centre for Subsurface Imaging, Institute of Hydrocarbon Recovery, Universiti Teknologi PETRONAS, Seri Iskandar 32610, Perak, Malaysia; [b]Department of Geology, School of Environmental Science and Natural Resources, Universiti Kebangsaan Malaysia, Bangi 43600, Selangor, Malaysia; [c]Digital Geoscience Global Sdn Bhd, Wilayah Persekutuan Kuala Lumpur 50400, Kuala Lumpur, Malaysia; [d]Engineering Geology, Institut Teknologi Sumatera, Jl. Terusah Ryacudu, Way Huwi, Kabupaten Lampung Selatan, Lampung 35365, Indonesia

Abstract The continuous development in the urbanisation, industrial, and agricultural sectors, coupled with an increase in the population of a given area, impacts the quality and supply of surface water. Groundwater serve as a viable alternative to mitigate these challenges. However, ensuring the safety and sustainability of groundwater necessitates comprehensive quality monitoring. This study employs statistical techniques and conventional plotting methods to evaluate the groundwater quality, physical properties, and chemical composition derived from 55 monitoring wells across the Muda River Basin Laboratory analyses reveal that the groundwater in the Muda River Basin exhibits alkaline characteristics, with electrical conductivity values ranging from 0 to 1050 µS/cm. The hydrogeochemical profile is primarily influenced by silicate and carbonate weathering processes, driven by the region's consistently humid and hot climatic conditions. Principal Component Analysis (PCA), accounting for 80.4% of the dataset's variance, identifies ion exchange, soil mineralization, silicate weathering, and carbonate dissolution as the dominant processes shaping groundwater chemistry. The study also determines the major ionic composition of groundwater in the following order: $HCO_3^- > Ca^{2+} > Na^+ > Cl^- > SO_4^{2-} > Mg^{2+} > NO_3^- > K^+$. The concentrations of these ions conform to the World Health Organization (WHO) standards for drinking water quality. The findings demonstrate that integrating multivariate statistical methods, conventional hydrochemical plots, and geochemical modeling is instrumental in elucidating the factors governing groundwater quality.

Keywords: Groundwater, hydrochemical assessment, Muda river basin.

Introduction

Groundwater serves as a crucial natural resource, providing water for drinking, irrigation, and industrial activities, with billions of people worldwide depending on it [1]. However, in recent years, concerns regarding groundwater quality deterioration have escalated due to extensive agricultural and urban development, as well as increasing population density, all of which adversely affect groundwater quality. The chemical composition of groundwater is influenced by various natural processes, including oxidation-reduction [2], dissolution-precipitation [3], and physical phenomena such as evaporation, mixing, and dispersion [4]. In addition, anthropogenic activities significantly contribute to alterations in groundwater chemistry [5].

Groundwater quality is closely tied to regional geology and aquifer characteristics, as it is shaped by both natural and human-induced factors. Hydrogeochemical processes, such as residence time, oxidation, precipitation, recharge and discharge dynamics, and ion exchange, play a critical role in determining the chemical properties of groundwater [6]. Groundwater interacting with an aquifer system is influenced by several factors, including the mineralogy of the aquifer, geological formations, flow direction, and the chemical properties of recharge zones [7, 8]. Furthermore, anthropogenic activities, such as fertilizer leaching, overextraction, and contamination from spills, have a negative impact on groundwater quality.

To better understand groundwater quality, various methodologies have been employed to assess its characteristics and the associated hydrochemical processes. These include multivariate statistical analyses [9, 10, 11], geochemical modelling [12, 13], stable isotope studies, and structural equation modelling [14], all of which provide insights into the geochemical evolution and hydrochemical mechanisms influencing groundwater composition in specific regions. In this study, groundwater quality and the underlying geochemical processes in the Muda River Basin, Kedah, Malaysia, were evaluated using multivariate techniques, geochemical modelling, and conventional graphical approaches to identify the key factors controlling groundwater quality.

Study Area

The Muda River Basin is located in the southern region of Kedah state, extending from northern Perak to the south and reaching northern Penang and southern Thailand in the west and north, respectively. The basin encompasses several districts, including Baling, Kuala Muda, Kulim, Padang Terap, Sik, and Pendang [15]. Geographically, the study area is positioned between latitudes 5°02'0"N and 6°01'0"N and longitudes 100°02'0"E and 101°01'0"E, covering an approximate area of 4,200 km² (Figure 1). Elevation within the basin varies significantly, ranging from lowland areas at 2.5–70 m to highland regions reaching up to 1,860 m above sea level. The climate is tropical, with an average annual temperature of 25.4°C. The region experiences a distinct dry season lasting four months (December–March) and a rainy season spanning eight months (April–November), with an average annual rainfall of 2,000–3,000 mm [16].

The Muda River Basin features three key sedimentary formations (Figure 2): Mahang (Lower Ordovician–Upper Devonian), Semanggol (Lower Permian–Upper Triassic), and Saiong (Jurassic–Cretaceous). The Main Range granite in the central region and the Bintang Range granite in the southeastern region together account for nearly half of the basin. The Mahang Formation, located in the southwest, consists of arenite and silicate facies, argillitic facies, and limestone facies [17]. This formation correlates with the Sungai Petani and Baling Formations, which are separated by a granite body [18]. The Semanggol Formation is characterized by conglomerate, rhythmic, and chert facies [19]. However, Foo [20] proposed that the southern portion of the Semanggol Formation in northern Perak contains only two dominant lithofacies, excluding the chert facies—a perspective corroborated by Sajid *et al.* [21]. The Saiong Beds, which unconformably overlie the Semanggol Formation [22], extend from northeast Kedah to southeastern Thailand. Additionally, the northwestern section of the basin contains several Kodiang limestone outcrops, which share a geological age with the Semanggol Formation [23,24,25,26,27].

Methodology

Sampling and Analysis

In January 2020, a total of 55 groundwater samples were systematically collected from monitoring wells within the Muda River Basin. This total includes 21 samples obtained from nearby areas with distinct geological formations, such as the Jerai and Kubang Pasu Formations, and regions with heightened agricultural activities, including paddy cultivation zones, to account for the influence of external factors. The samples were analyzed to determine several physical and chemical parameters, including pH, electrical conductivity (EC), and total dissolved solids (TDS). These parameters were measured using portable field equipment, specifically a pH meter, an EC electrode (Oakton), and a TDS meter (HANNA), respectively. To ensure the integrity of the samples, they were stored in an ice box at a constant temperature of 4℃ and promptly transported to the laboratory for detailed chemical analysis.

For cation analysis, the groundwater samples were acidified to a pH of less than 2 using 50% nitric acid, while samples intended for anion analysis were kept unaltered to preserve their natural composition. Major cations, including Mg^{2+}, Ca^{2+}, Na^+, and K^+, as well as iron (Fe), were analyzed using an atomic absorption spectrometer (Thermo Fisher Scientific M series). Anions, such as F^-, Cl^-, SO_4^{2-}, and NO_3^-, were quantified using an ion chromatograph (Dionex). Additionally, the total alkalinity and hardness of the groundwater samples were determined using the titrimetric method [28].

After completing the chemical analysis of all groundwater quality parameters, the normalised charged balance index (NCBI) was calculated to assess the ionic balance in the groundwater samples. The NCBI was determined using the following formula [29, 30]:

$$NCBI = [(\sum T_z{}^- - \sum T_z{}^+) / (\sum T_z{}^- + \sum T_z{}+)] \times 100$$

Where $\sum TZ+$ represents the total sum of cations (in epm), and $\sum TZ-$ represents the total sum of anions (in epm). The calculated NCBI values for the groundwater samples ranged between -7.5% and 7.5%, indicating an acceptable range of ionic balance, as per established guidelines.
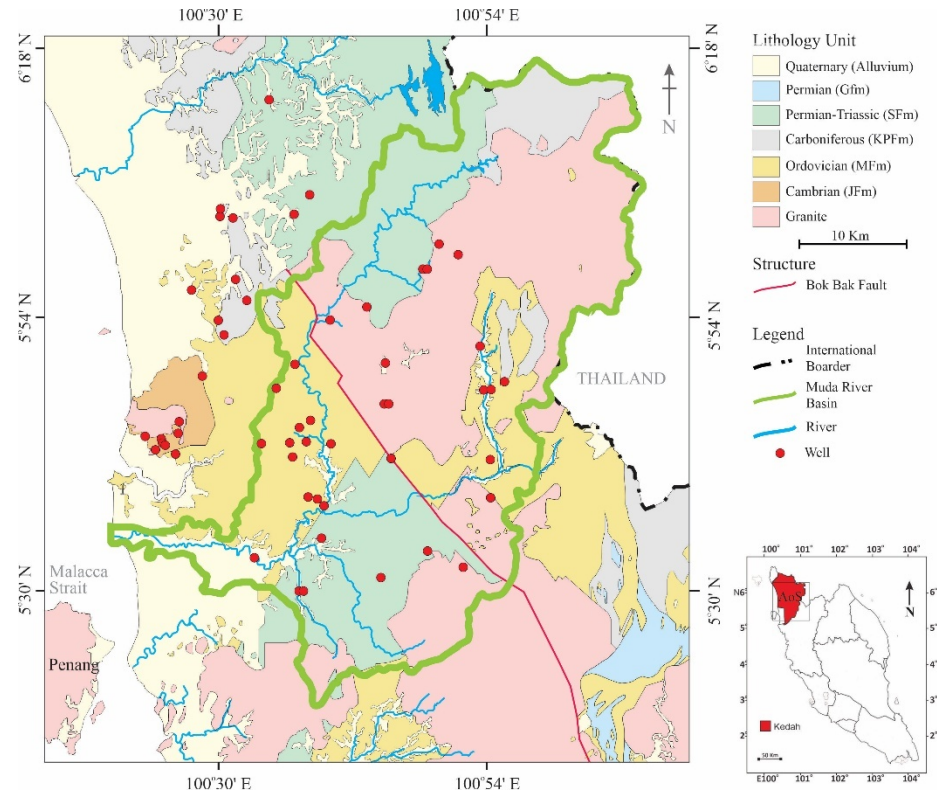
Figure 1. Base map of the Muda River Basin in Kedah, Malaysia. The red dots represent groundwatermonitoring wells. Additionally, 21 wells located outside the northwestern part of the Muda River Basin were included to establish a comprehensive correlation with the surrounding geology

Statistical Analysis

A comprehensive correlation analysis of groundwater quality parameters was conducted to better understand the interrelationships among the various measured parameters. The correlation coefficient (*r*) was used to quantify the strength and direction of these relationships, with *r* values ranging from -1 to +1. Variables with *r* > 0.7 were classified as having a strong positive correlation, indicating a significant linear relationship. Conversely, variables with *r* values between 0.5 and 0.7 were considered to exhibit a moderate correlation, suggesting a less pronounced but notable association between them. To minimize redundancy and extract meaningful patterns from the dataset, multivariate statistical techniques, such as principal component analysis (PCA), were employed. PCA is particularly effective in handling large datasets by reducing dimensionality while retaining the maximum amount of variance [31]. The PCA analysis was performed using the XLSTAT extension in Microsoft Excel. As part of the process, Bartlett's sphericity test was conducted on normalized data to evaluate its suitability for PCA.

The results of Bartlett's test revealed that the calculated chi-square value ($X^2cal =1190.4$) exceeded the critical chi-square value ($X^2crit = 202.5$) at a degree of freedom of 171, a significance level of 0.05, and a p- value of 1. This outcome confirmed that the dataset was adequately structured for PCA, enabling effective interpretation and identification of the underlying relationships among the groundwater quality parameters [32]. The use of PCA not only simplified the dataset but also highlighted the key factors controlling the variation in groundwater quality within the study area.

Geospatial Database

To evaluate the spatial distribution of groundwater quality parameters within the study area, advanced geospatial analysis tools, specifically ArcGIS 10.8, were utilized. Spatial interpolation techniques were applied to point data collected from groundwater sampling sites to create a continuous surface representation of the data. Among the various interpolation methods available, the inverse distance weighted (IDW) algorithm was employed for this purpose. IDW is particularly suitable for analyzing geospatial datasets as it assumes that points closer to one another have a stronger influence on the interpolated values, resulting in a more accurate representation of spatial variability. The flexibility of the IDW method makes it an effective tool for generating surface maps that allow for detailed visualization of different spatial geometries, including areas, volumes, and linear features. It also supports the use of various power functions, such as linear, squared, and cubic, which can be adapted to suit the specific distribution and behavior of the data. By leveraging these capabilities, surface maps for groundwater quality parameters, such as pH, electrical conductivity (EC), total hardness (THD), and major cations and anions, were produced. These maps provided critical insights into the spatial patterns and variability of groundwater quality across the study area, enabling a deeper understanding of the factors influencing the distribution of these parameters. The integration of geospatial tools with interpolation techniques facilitated comprehensive analysis and effective visualization, which are essential for groundwater quality assessment and management.

Results and Discussion

Distribution of Major Ions

The geochemical processes inside the aquifer system and the interactions between rocks and water affect the chemical properties of groundwater. Table 1 presents the general statistics of the analysed groundwater quality parameters and the baseline limits established by the World Health Organization (WHO) and Ministry of Health (MoH).

Table 1. Table of groundwater hydro-physicochemical descriptors with World Health Organization (WHO) Guidelines of groundwater quality parameters

Parameter	Unit	Min (SD)	WHO	MoH
pH	-	7.47 ± 0.67	6.5-8.5	6.5-9.0
TSS	mg/L	140.74 ± 107.63	-	-
EC	µS/m	199.35 ± 167.78	-	-
TDS	mg/L	87.85 ± 79.74	500	1000
HCO_3^-	mg/L	85.57 ± 71.87	500	-
Cl^-	mg/L	9.48 ± 30.7	500	250
SO_2^{4-}	mg/L	5.14 ± 8.15	250	250
NO_3^-	mg/L	2.67 ± 4.53		
Ca^{2+}	mg/L	16.33 ± 16.38	250	-
Mg^{2+}	mg/L	3.93 ± 4.54	75	150
K^+	mg/L	1.86 ± 2.64	-	-
Na^+	mg/L	11.06 ± 31.5	200	200
Fe	mg/L	2.10 ± 4.92	NA	0.3
Mn	mg/L	0.29 ± 0.5	NA	0.1
As	mg/L	0.01 ± 0.01	0.01	0.01
Cu	mg/L	0.20 ± 0.674	2	1
Pb	mg/L	0.01 ± 0.0056	0.01	0.01
Zn	mg/L	0.14 ± 0.178	NA	3
F	mg/L	0.80 ± 1.361	0.07	0.02
Cd	mg/L	0.02 ± 0.012	0.003	0.003
Se	mg/L	0.01 ± 5.25	0.04	0.01
Cr	mg/L	0.01 ± 5.25	0.04	0.05
SiO_2	mg/L	24.19 ± 19.53		

SD = Standard Deviation, WHO = World Health Organization MoH = Ministry of Health

pH

Figure 2a shows the pH distribution in Muda River Basin. The pH values of groundwater samples in the study area range from 6.5 to 8, with an average of 7.45. Notably, the groundwater pH falls within the baseline limits established by the WHO. Among the 57 groundwater samples analyzed, only 14 exhibit a pH value below 7, indicating a significant interaction between soil and water, contributing to the high alkalinity of the aquifers. The distribution of low pH values is more concentrated in the southwestern region, identified as an area with low to moderate topography and composed of sedimentary formations, namely the Semanggol and Mahang Formations. The pH values are remarkably lower in the Semanggol Formation compared to the Mahang Formation, whereas areas characterized by higher topography and granite bedrock exhibit higher pH levels. These variations may be attributed to anthropogenic activities such as sewage disposal and fertilizer application in densely populated coastal areas with low topography. These activities, combined with natural phenomena such as brackish water intrusion into sandy aquifers, are believed to initiate subsurface geological weathering processes affecting the southwestern part of the study area.

Electrical Conductivity (EC)

Based on Figure 2b, the electrical conductivity (EC) values in the Muda River Basin range from 0 to 1050 µS/cm (Figure 2b), aligning with the national groundwater quality guidelines for conventional drinking water treatment (<1000 µS/cm) set by the Department of Environment, Malaysia (DOE). Higher EC values observed in the southwestern part of the study area indicate salt enrichment in the groundwater, corresponding to the estuary of the Muda River, which merges with the Straits of Malacca. Approximately 96% of the area surrounding the Muda River Basin falls within the range classified as freshwater (0–800 µS/cm) as proposed by the WHO, despite the upper limit being set at 1500 µS/cm. Nearly 85% of the EC distribution from the northeast to the south of the basin is classified as excellent (<250 µS/cm), 11% as very good (250–750 µS/cm), with the remainder permissible for drinking within certain thresholds.

Total Dissolved Solids (TDS)

The total dissolved solids (TDS) values in the Muda River Basin in Figure 2c, ranges from 9.3 mg/L to 520 mg/L (Figure 2c, also complying with the national groundwater quality guidelines for conventional drinking water treatment (<1500 mg/L) issued by the DOE. With an average TDS of 88.12 mg/L, the groundwater remains well below the maximum permissible limit of 1000 mg/L recommended by the WHO. According to the groundwater classification by Davis and De Wiest (1966), TDS levels of <500 mg/L, 500–1000 mg/L, and >1000 mg/L correspond to probabilities of 82%, 14%, and 4%, respectively, for drinking and irrigation suitability. TDS values below 1000 mg/L are classified as freshwater, and the range and distribution of TDS within the Muda River Basin indicate that all areas are suitable for drinking water purposes. The physical properties of groundwater indicates a strong relationship between pH, EC, and TDS, particularly in terms of their average distribution patterns. The relationship between EC and TDS is more pronounced compared to pH, as evidenced by the consistent distribution trends across the study area. This suggests that EC and TDS are interdependent and are both influenced by the ionic composition and dissolved salts in the groundwater, which vary spatially across the basin.

Major Cations

The major cations in the Muda River Basin are dominated by calcium (Ca^{2+}), followed by sodium (Na^+), potassium (K^+), and magnesium (Mg^{2+}). Ca^{2+} concentrations in Figure 2d, ranges from 0.5 mg/L to 93 mg/L, with the highest values primarily attributed to chemical weathering processes involving limestone, particularly from the Kubang Pasu Formation in the northern part of the basin. Figure 2e shows Na^+ concentrations that vary from 0 mg/L to 280 mg/L, with an average of 11.95 mg/L, which is consistent with the WHO guideline of 200 mg/L for groundwater quality. Elevated Na^+ concentrations, especially in the northwestern region, are likely due to the intrusion of saline or brackish water from the nearby Malacca Strait. K^+ (Figure 2f) which ranges from 0 mg/L to 26 mg/L and averages 1.93 mg/L, shows relatively low concentrations. This is likely because potassium-bearing minerals, such as potash feldspar, are more resistant to chemical weathering, resulting in slower release of potassium ions, except in localized areas near the contact between the Semanggol Formation and granite. Figure 2g exhibit Mg^{2+} concentrations in the Muda River Basin that range from 0 mg/L to 35 mg/L, with an average of 3.92 mg/L, and are influenced by chemical weathering, especially the decomposition of dolomite, although the absence of dolomite in the study area suggests contributions from clay minerals and metamorphic rocks.

Major Anions

the dominant major anion is bicarbonate (HCO_3^-), with concentrations ranging from 2.6 mg/L to 333 mg/L and an average of 123.03 mg/L as shown in Figure 2h. This high average is attributed to the weathering of carbonate minerals and silicates, as well as the decomposition of organic matter. Elevated HCO_3^- levels are particularly linked to the Kubang Pasu Formation in the northern basin and limestone

facies of the Mahang Formation. Other anions, such as chloride (Cl^-), sulfate (SO_4^{2-}), nitrate (NO_3^-), and fluoride (F^-), are present in lower concentrations. Cl^- concentrations (Figure 2i) ranges from 0 mg/L to 200 mg/L (average 9.06 mg/L), with higher levels observed in wells PK45, suggesting saline water intrusion. SO_4^{2-} concentrations (Figure 2j) are also low, ranging from 0 mg/L to 23 mg/L, and are linked to the weathering of sulfate-bearing minerals such as gypsum. NO_3^- concentrations (Figure 2k), ranging from 0 mg/L to 15 mg/L, show occasional spikes likely due to agricultural runoff (palm and rubber plantation) and sewage infiltration, especially in areas of the Semanggol and Mahang Formations. Lastly, F^- levels (Figure 2l), ranging from 0.5 mg/L to 9.5 mg/L, exceed the WHO guideline in some boreholes near granite and Mahang Formation contact zones. Overall, the concentrations of major anions in the Muda River Basin are within safe limits, except for some localized anomalies. Three wells, PK45, PK427, and PK447, have been identified as having at least one major anion exceeding the WHO guideline. All three wells exhibit elevated F^- concentrations, while PK45 also shows high levels of K^+ and Cl^-. The elevated F^- concentrations observed in all three wells are attributed to the weathering of granitic bedrock in contact with the Mahang Formation. High K^+ levels result from intensified chemical weathering of potassium-bearing minerals, such as potash feldspar, near the contact zone between the Semanggol Formation and granite. Cl^- levels indicate potential saline water intrusion, likely from proximity to coastal areas or historical seawater influence.

Association between Water Quality Parameters

Statistical Analysis

The correlation analysis in Table 2 shows strong positive relationships between electrical conductivity (EC), total dissolved solids (TDS), bicarbonate (HCO^{3-}), and calcium (Ca^+), with correlation coefficients exceeding 0.8. These high correlations suggest that these variables are strongly interrelated and likely influenced by processes such as the dissolution of salts and carbonates, which contribute to the ionic strength of the water. On the contrary, some variables, such as chloride (Cl^-) and nitrate (NO_3^-), exhibit negative or weak correlations with other parameters, indicating distinct hydrochemical processes. For instance, chloride's weak correlations may reflect its conservative behavior, while nitrate may indicate influences from anthropogenic sources, such as agricultural runoff. Other variables, such as potassium (K^+), display generally weak correlations, implying a minimal contribution to major hydrochemical patterns.

PCA provides further understandings by reducing the complexity of the dataset into five principal components as shown in Table 3 with eigenvalues greater than 1, collectively explaining 82.32% of the total variance. The first principal component (PC1) explains 31.83% of the variance and is dominated by high positive loadings of EC (0.4445), TDS (0.1021), HCO^{3-}, and Ca^+. This suggests that PC1 represents the overall salinity or ionic strength of the water, driven by the dissolution of salts and carbonate minerals. The second principal component (PC2), which accounts for 21.49% of the variance, is characterized by a strong positive loading of sulfate (SO_4^{2-}) at 0.7556, along with contributions from magnesium (Mg^+). This component likely reflects sulfate-related processes, such as dissolution of gypsum or pollution from industrial and agricultural sources. The third principal component (PC3), explaining 11.63% of the variance, is distinguished by a strong negative loading for fluoride (F^-) at -0.8518. This indicates that fluoride concentrations are influenced by a distinct process, possibly associated with geogenic sources such as the weathering of fluorapatite. The fourth and fifth components (PC4 and PC5), explaining 8.98% and 8.39% of the variance respectively, capture more specific trends. PC4 is associated with Ca^+ (0.5535) and may represent carbonate weathering or contributions from groundwater flow through limestone formations. Meanwhile, PC5 is characterized by negative loadings for NO_3^- (-0.5515) and positive contributions from K^+ (0.3994), suggesting influences from agricultural runoff or biological activity affecting nutrient dynamics. The relationships between the correlation matrix and PCA findings demonstrate how highly correlated variables cluster within the same principal components. For example, EC, TDS, HCO^{3-}, and Ca^+ dominate PC1 due to their strong interrelationships in the correlation matrix. Similarly, SO_4^{2-} and Mg^+ contribute significantly to PC2, representing a different hydrochemical process.
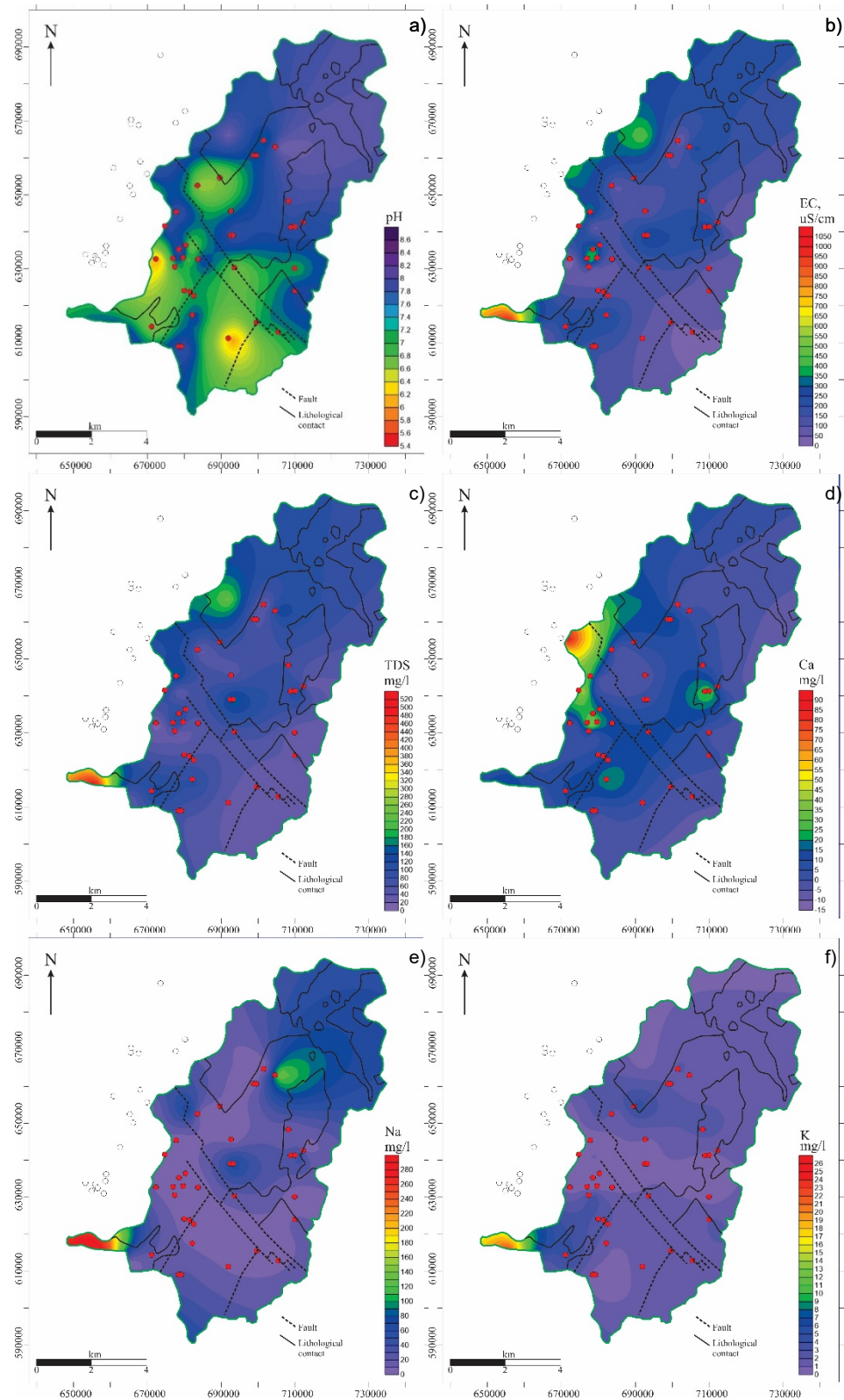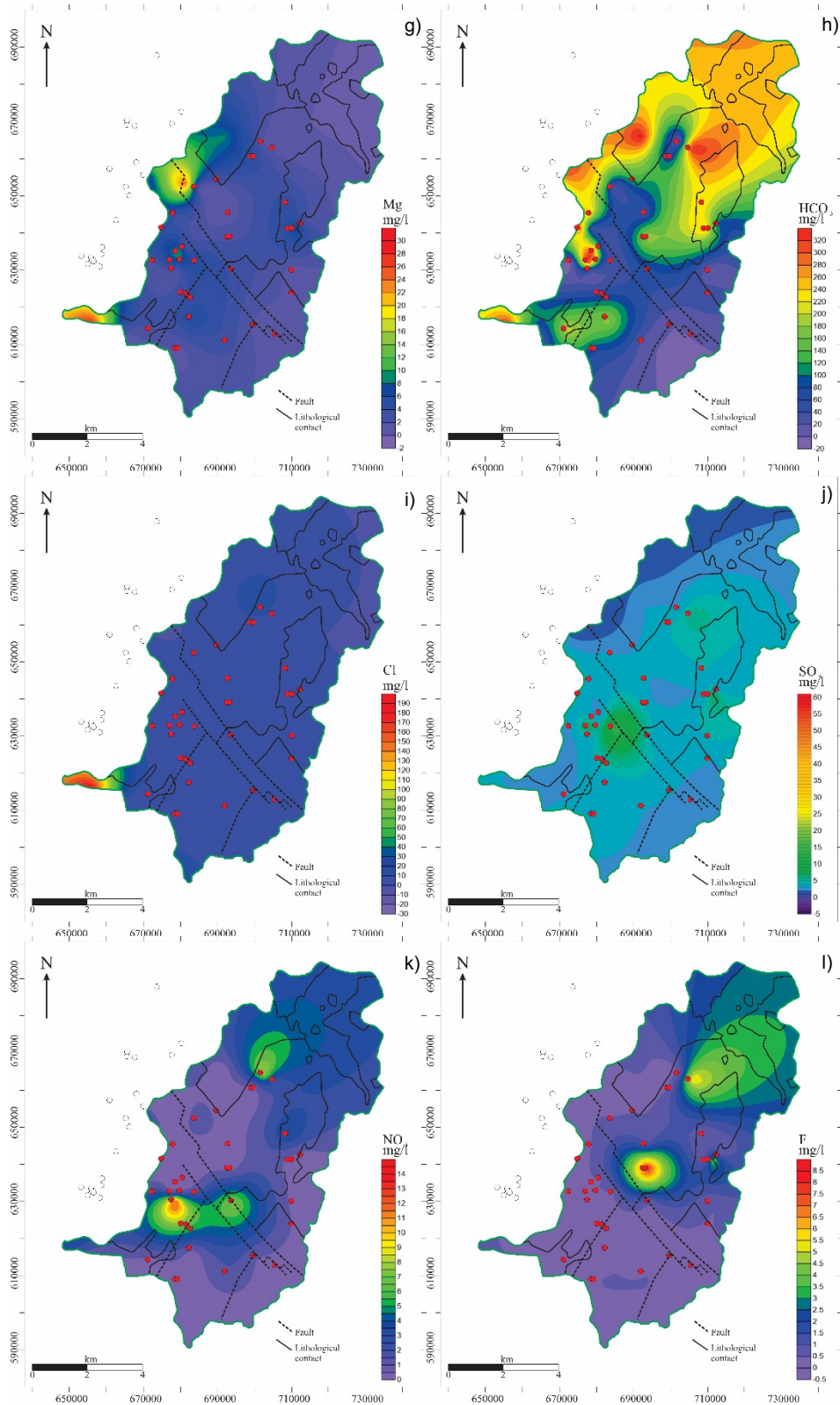
Figure 2. Distribution map of a) pH, b) electrical conductivity, c) total dissolved solid, d) calcium e) Sodium, f) Potassium g) magnesium, h) bicarbonate, i) chloride, j) sulphate, k) nitrate, l) floride. (red dots represent the groundwater sampling locations)

Table 2. Correlation analysis of groundwater quality parameters (bold letters indicate a strong relationship between the variables)

Variables	EC	TDS	pH	Na	K	Ca	Mg	Cl	SO₄	HCO	NO₃	F	SiO₂	Fe
EC	**1**													
TDS	**0.917**	**1**												
pH	**0.581**	**0.594**	**1**											
Na	0.266	**0.399**	**0.320**	**1**										
K	-0.097	0.020	-0.093	0.215	**1**									
Ca	**0.682**	**0.525**	**0.371**	0.092	-0.004	**1**								
Mg	**0.470**	**0.475**	**0.275**	0.265	0.151	**0.480**	**1**							
Cl	0.070	0.134	-0.116	**-0.709**	0.009	0.057	**0.269**	**1**						
SO₄	0.080	0.123	-0.129	-0.029	-0.051	0.077	**0.296**	**0.951**	**1**					
HCO₃	**0.925**	**0.845**	**0.671**	**0.360**	-0.062	**0.650**	**0.420**	-0.116	-0.099	**1**				
NO₃	**-0.313**	**-0.310**	**-0.317**	-0.100	0.159	**-0.288**	-0.252	-0.039	**-0.068**	**-0.368**	**1**			
F	0.209	**0.312**	**0.288**	**0.690**	-0.128	-0.079	-0.055	-0.006	0.008	0.215	-0.073	**1**		
SiO₂	0.221	**0.287**	0.179	0.077	0.123	0.012	0.026	-0.072	-0.082	0.209	-0.205	0.022	**1**	
Fe	0.092	0.078	-0.073	**-0.107**	0.026	0.071	**0.328**	**0.764**	**0.759**	-0.021	-0.155	-0.076	-0.14	**1**

Table 3. Loading factors along with Eigen-values varieties %, variance %, and cumulative % (bold letters indicate significant loadings on the variables)

Variable	PC1	PC2	PC3	PC4	PC5
EC	**0.4445**	0.4372	0.3399	0.2071	-0.0143
TDS	0.1021	0.0031	-0.1088	-0.3127	-0.0122
pH	0.076	-0.0744	-0.0116	-0.5025	-0.2109
Na	0.071	0.0634	0.1932	-0.2033	**-0.6676**
K	0.0779	0.137	0.0559	-0.1434	**0.3994**
Ca	0.0127	-0.1124	0.0141	**0.5535**	-0.1086
Mg	0.2336	0.1153	0.0189	-0.271	-0.0111
Cl	**-0.6262**	-0.0401	-0.1293	-0.07	-0.0815
SO4	-0.4515	**0.7556**	0.0648	0.0316	-0.0787
HCO3	-0.165	0.1357	-0.061	0.1625	0.0287
NO3	0.0389	-0.1078	-0.1836	0.2829	-0.5515
F	0.2108	0.1892	**-0.8518**	0.0374	0.0287
SiO2	0.2208	0.3404	-0.2175	-0.0669	-0.1309
Fe	0.1124	-0.0161	0.0109	0.2165	0.0468
Eigen Value	4.456	3.009	1.628	1.257	1.174
Variability (%)	31.83	21.49	11.63	8.98	8.39
Cumulative %	31.83	53.32	64.95	73.93	82.32

Independent variables, such as F⁻ and NO₃⁻, show weak correlations with other variables and, thus, form distinct components (PC3 and PC5). PC1 highlights general salinity and ionic strength, PC2 emphasizes sulfate-related processes, and subsequent components capture more specific factors such as fluoride and nutrient dynamics.

Hydro-Geochemical Process

Weathering and Dissolution

The distribution plots in Figure 3 explain the geochemical processes governing groundwater composition in the Muda River Basin, Kedah, Malaysia, in relation to its underlying lithological units. Figure 3(a) presents the relationship between divalent cations ($Ca^{2+} + Mg^{2+}$) and the sum of HCO_3^- and SO_4^{2-}. The majority of the data points are situated below the equilibrium line, indicating that silicate weathering is the dominant process releasing Ca^{2+} and Mg^{2+} into the groundwater. This is primarily attributed to the breakdown of silicate minerals, such as feldspars and pyroxenes, in the granitic and sedimentary lithologies of the Semanggol Formation. While carbonate weathering also contributes to groundwater chemistry, its influence is secondary, as evidenced by localized clusters of points closer to the carbonate weathering zone. These contributions are likely derived from the dissolution of carbonate minerals in the Mahang Formation, particularly in the northwestern part of the basin, where carbonate lithologies are prevalent

Figure 3b illustrates the relationship between HCO_3^- and Na^+, further elucidating the geochemical processes shaping groundwater chemistry. Elevated concentrations of HCO_3^- reflect the dominance of silicate weathering, facilitated by the reaction of carbonic acid with silicate minerals. Simultaneously, elevated Na^+ levels are indicative of multiple sources, including the dissolution of sodium-bearing minerals such as albite and the weathering of granitic rocks. Coastal influences and minor evaporite dissolution also contribute to Na^+ in localized regions. The observed Na/Cl ratio greater than 1 reinforces the preeminence of silicate weathering, as Na^+ release through mineral weathering outweighs Cl^- contributions from evaporites or seawater intrusion. Additionally, the higher HCO_3^- to Na^+ ratio aligns with bicarbonate enrichment due to silicate weathering, consistent with findings in silicate-dominated terrains.

Figure 3c, which plots Mg/Na against Ca/Na, underscores the significance of silicate weathering in the basin. The clustering of data points in the weathered silicate region indicates that silicate weathering processes, likely associated with the Semanggol Formation and granite outcrops, are the primary sources of groundwater solutes. A limited number of points extending into the carbonate weathering zone suggest localized carbonate dissolution, particularly in areas underlain by the Mahang Formation. These trends may also reflect the mixing of waters influenced by silicate weathering with minor contributions from carbonate weathering or evaporite dissolution.

Figure 3d examines the relationship between HCO_3^-/Na^+ and Ca_2^+/Na^+, further substantiating the dominance of silicate weathering. Elevated bicarbonate concentrations, relative to sodium, highlight the significant contribution of carbonic acid-driven silicate weathering reactions. The data points predominantly align with the silicate weathering region, with a smaller subset indicative of carbonate dissolution. The latter corresponds to areas influenced by carbonate lithologies, such as those found in the Mahang Formation. This localized influence of carbonate weathering is most prominent in the northwestern portion of the basin, where the Mahang Formation is spatially distributed.

The geochemical composition of groundwater in the Muda River Basin reflects the interplay between silicate and carbonate weathering, driven by the basin's lithological diversity. Granite outcrops, with their feldspar-rich mineralogy, contribute significantly to the silicate weathering process, releasing $Na+$, HCO_3^-, and K^+. The Semanggol Formation, characterized by sedimentary rocks such as sandstone and shale, further amplifies silicate weathering through the breakdown of silicate minerals, releasing divalent and monovalent cations. Meanwhile, the Mahang Formation, consisting of carbonate-rich lithologies, enhances localized contributions of Ca^{2+}, Mg^{2+}, and HCO_3^-, particularly in regions with carbonate outcrops. Overall, the ionic composition of groundwater in the Muda River Basin characterized by the order $HCO_3^- > Ca^{2+} > Na^+ > Cl^- > SO_4^{2-} > Mg^{2+} > NO_3^- > K^+$ is primarily controlled by silicate weathering. Carbonate weathering exerts a secondary but localized influence, particularly in areas underlain by the Mahang Formation. These hydrochemical trends underscore the critical role of lithology in regulating groundwater geochemistry, with silicate weathering dominating across the basin, supplemented by localized contributions from carbonate dissolution and minor evaporite interactions. The observed patterns highlight the complex geochemical interactions shaped by the interplay between lithological heterogeneity and weathering processes in the Muda River Basin.
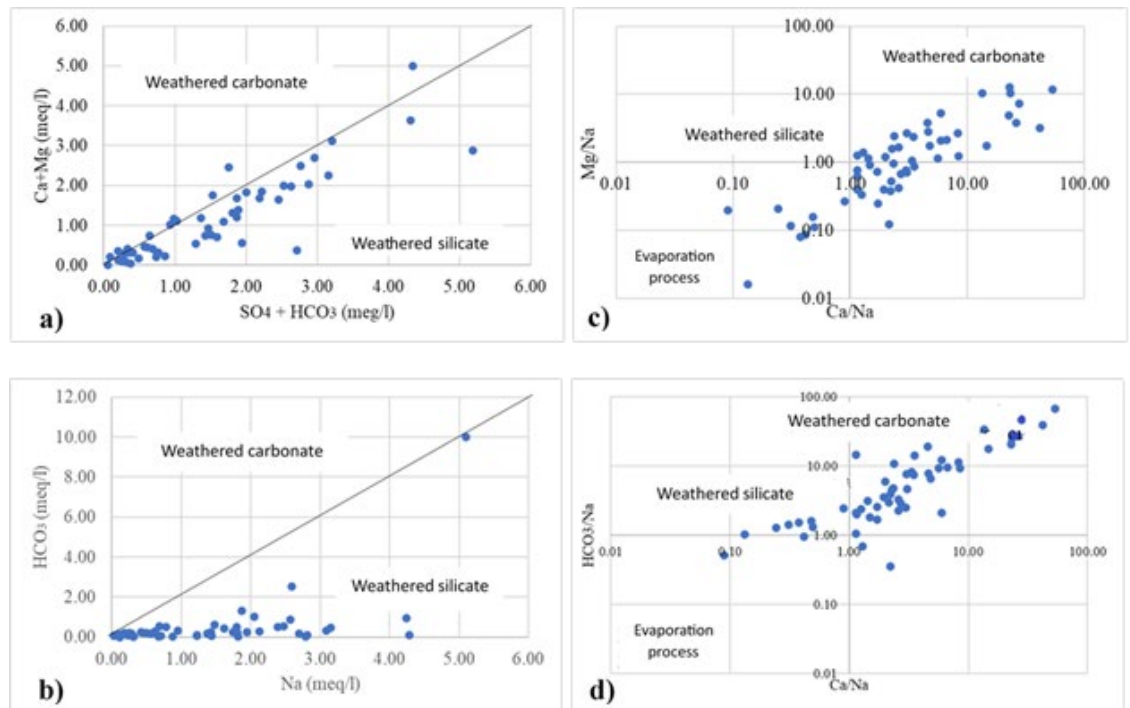
Figure 3. a) Distribution plot of Ca + Mg vs SO_4 + HCO_3, b) Distribution of HCO_3 vs Na, c) Distribution plot of Mg/Na vs Ca/Na, d) Distribution plot of HCO_3/Na vs Ca/Na

Geochemical Modelling

Geochemical Facies

The trilinear Piper diagram presented in Figure 4 illustrates the groundwater geochemical composition derived from 55 wells in the Muda River Basin. The analysis reveals that Ca is the dominant cation species, followed by Na + K and Mg, while HCO_3 is the dominant anion species, followed by Cl and SO_4. This suggests that carbonate dissolution processes dominate the geochemical characteristics of the groundwater in the basin. The results indicate that the most prevalent water type in the study area is Ca-HCO_3, comprising 75% of the groundwater samples. Other water types include Ca-Na-HCO_3 (8%), Ca-Mg-Cl (7%), NaHCO_3 (5%), and minor occurrences of CaCl and NaCl. The dominance of the Ca-HCO_3 type reflects natural carbonate dissolution processes, likely from the interaction of water with carbonate minerals such as calcite ($CaCO_3$) or dolomite ($CaMg(CO_3)_2$), coupled with CO_2 absorption from the atmosphere and soil zones. The presence of mixed and minor water types suggests localized processes such as ion exchange, halite dissolution, or anthropogenic inputs.

The spatial distribution of groundwater geochemical sequences, as shown in Figure 5, further highlights the processes influencing groundwater chemistry in the Muda River Basin. The Ca-HCO_3 water type is widely distributed across the study area, with occurrences scattered across diverse lithological and topographical settings, consistent with widespread carbonate dissolution. In contrast, the Ca-Na-HCO_3 and Ca-Mg-Cl water types exhibit clustered distributions, with the former concentrated at the foothills of Gunung Jerai and the latter in the southwestern region of the basin. Gunung Jerai, likely a recharge area, may contribute to mixed sequences through the interaction of groundwater with granitic and sedimentary formations. The southwest region, dominated by paddy cultivation, suggests anthropogenic influences such as fertilizer application contributing to elevated Ca-Mg-Cl concentrations. Additionally, isolated wells representing NaHCO_3 exhibit a linear distribution along a southeast-northwest axis, potentially indicating the influence of structural controls such as faults or lithological boundaries. This alignment, spanning wells in granitic and sedimentary formations of the Semanggol Formation, further supports the hypothesis of geological or hydrological pathways affecting groundwater flow and composition.

The rare occurrences of NaCl and CaCl water types, represented by a single well each, appear to reflect specific localized processes. The CaCl water type, observed in well PP45 near Muara Sungai, likely

results from halite dissolution or seawater intrusion in the coastal area. Similarly, the NaCl water type in the western basin may reflect anthropogenic contamination or unique geological features. The dominance of Ca in the groundwater is likely driven by cation exchange processes, where Na and K are replaced by Ca and Mg adsorbed onto clay mineral surfaces. Furthermore, the elevated HCO_3 concentrations reflect the dissolution of CO_2 and carbonate minerals during sedimentation and infiltration processes, contributing to the observed bicarbonate-dominated facies. The clustering of Ca-Mg-Cl sequences in agricultural zones indicates anthropogenic influences, while the geochemical variability associated with $NaHCO_3$ and mixed water types suggests the role of lithological differences and structural controls in shaping groundwater chemistry.

Gibbs Plot

The Gibbs diagram in Figure 6 provides insights into the mechanisms controlling the groundwater chemistry in the Muda River Basin. Based on the plots of (Ca+Na)/(Ca+Na+K) and Cl/(Cl+HCO_3) against total dissolved solids (TDS), it appears that no single dominant mechanism governs the chemical composition of the groundwater. Instead, the geochemical characteristics suggest that rock weathering processes are the primary drivers for the observed anion composition, particularly due to the abundance of HCO_3 in the groundwater. The presence of HCO_3 is a key indicator of carbonate dissolution, a typical outcome of rock weathering in regions dominated by carbonate or silicate lithologies. This observation aligns with the dissolution of minerals such as calcite, dolomite, and feldspars contributing to the groundwater composition.

While the anion composition appears largely influenced by rock weathering, the concentrations of groundwater cations seem to be shaped by additional factors, including lithology and anthropogenic activities. The (Ca+Na)/(Ca+Na+K) plot indicates that some samples deviate from the expected patterns for purely natural processes, implying the influence of human activities or localized lithological variability. Anthropogenic contributions, particularly from agricultural and urban activities, likely elevate the concentrations of ions such as Cl and HCO_3 in specific wells (*e.g.*, PP45, PK413, PK414, PK419, and PK443). The elevated Cl concentrations in these wells could be linked to processes such as halite dissolution, fertilizer application, or contamination from anthropogenic sources. The alignment of certain samples outside the typical Gibbs fields further reinforces the likelihood of anthropogenic influence on groundwater chemistry.

Although anthropogenic factors play a role in shaping the groundwater composition, the ionic mechanisms remain predominantly balanced within acceptable limits. This balance suggests that while human activities contribute to elevated concentrations of specific ions, the overall geochemical processes, such as ion exchange and rock weathering, still dominate the system. Furthermore, the consistent presence of HCO_3, along with moderate Cl levels, indicates that sedimentation and recharge processes also play a significant role in groundwater chemistry. The high TDS concentrations observed in some wells reflect localized zones of higher mineral dissolution or anthropogenic impact, consistent with the spatial variability in the Muda River Basin.

In conclusion, the Gibbs diagram highlights the interplay between natural geochemical processes and anthropogenic activities in controlling the groundwater chemistry of the Muda River Basin. Rock weathering, particularly the dissolution of carbonate and silicate minerals, remains the dominant mechanism influencing anion composition, while localized lithological and human-induced factors contribute to variations in cation and anion concentrations. The results underscore the importance of integrating both natural and anthropogenic factors when evaluating groundwater quality and its controlling mechanisms.
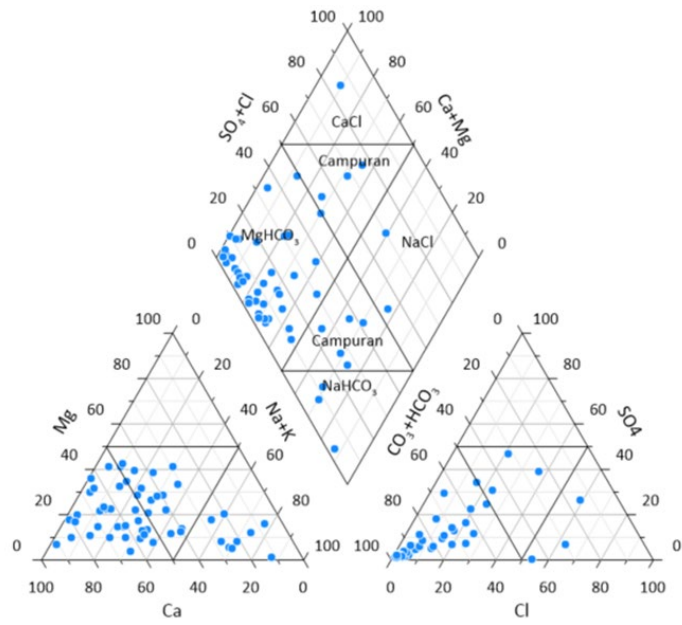
Figure 4. Piper analysis of groundwater geochemical sequence in Muda River Basin
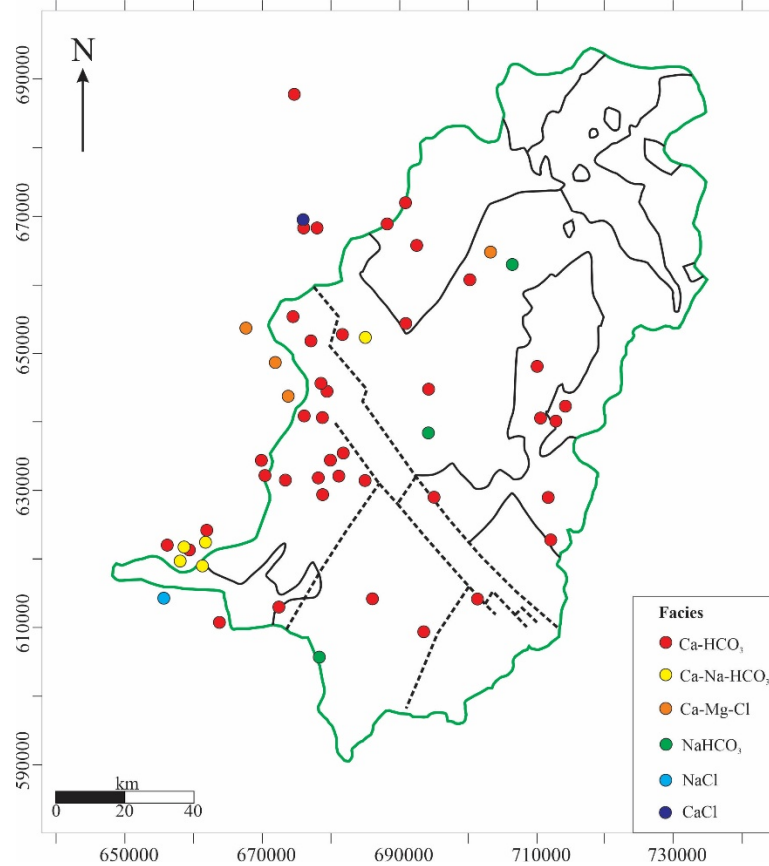
Figure 5. Distribution of groundwater geochemical sequence in Muda River Basin
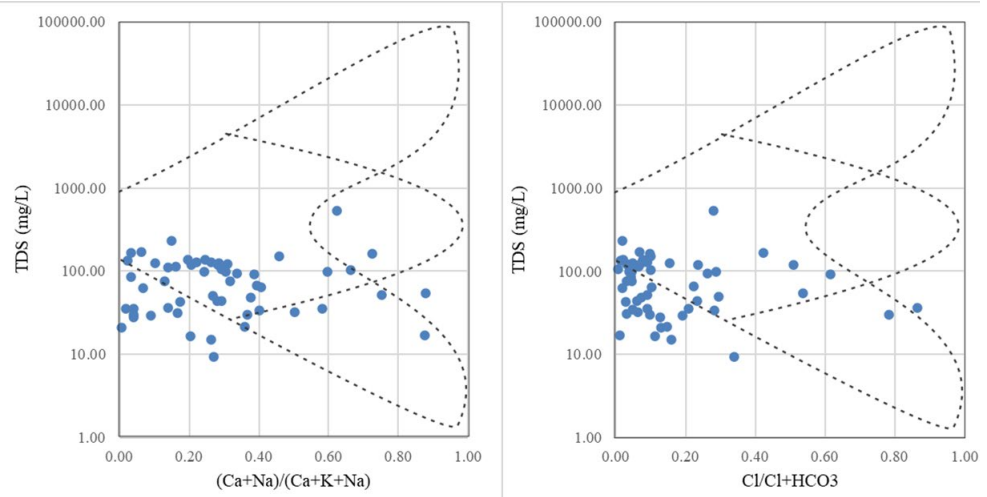
Figure 6. The Gibbs plot of (a) anion and (b) cation depicts the chemical mechanism of groundwater

Conclusion

In conclusion, the geochemical characteristics of groundwater in the Muda River Basin are influenced by a combination of natural processes, such as silicate and carbonate weathering, and localized anthropogenic activities. The dominant groundwater composition is characterized by calcium (Ca^{2+}) and bicarbonate (HCO_3^-), reflecting the dissolution of carbonate minerals like calcite and dolomite. Silicate weathering, primarily from granitic and sedimentary lithologies, contributes significantly to the ionic composition, releasing divalent cations such as calcium and magnesium. Elevated sodium concentrations, particularly in coastal and agricultural areas, indicate potential saline water intrusion and the influence of agricultural runoff. Statistical analyses and principal component analysis (PCA) further emphasize the interrelationship between electrical conductivity (EC), total dissolved solids (TDS), and major ions like calcium and bicarbonate. These results support the hypothesis that groundwater quality is primarily shaped by the dissolution of salts and carbonates, with minor contributions from anthropogenic factors like fertilizer application. The groundwater in the study area generally falls within the World Health Organization (WHO) guidelines for drinking water, although localized anomalies such as elevated fluoride (F^-) concentrations in certain wells and the occurrence of mixed water types suggest additional localized geochemical and anthropogenic influences. Overall, the findings underline the importance of understanding the interplay between geological factors and human activities in shaping groundwater quality. The distribution patterns of water types across the basin reflect both natural geochemical processes and the impacts of land use, such as agricultural activities and urbanization. As such, ongoing monitoring of groundwater quality is essential to ensuring safe water resources for the population while accounting for the evolving influences of both natural and anthropogenic factors.

Conflicts of Interest

The authors declare that there is no conflict of interest regarding the publication of this paper.

Acknowledgement

References

[1]   Connor, R. (2015). *The United Nations world water development report, 2015: Water for sustainable world* (Vol. 1). UNESCO Publishing.

[2]   Isa, N. M., Aris, A. Z., & Sulaiman, W. N. A. W. (2012). Extent and severity of groundwater contamination based on hydrochemistry mechanism of sandy tropical coastal aquifer. *Science of the Total Environment, 438*, 414–425.

[3]   Amiri, V., Sohrabi, N., & Dadgar, M. A. (2015). Evaluation of groundwater chemistry and its suitability for drinking and agricultural use in Lenjanat.

[4]   Polemio, M., Dragone, V., & Limoni, P. P. (2006). Salt contamination in Apulian aquifer: Spatial and time trend. In *Proceedings of 1st SWIM-SWICA* (19th Saltwater Intrusion).

[5]   Giridharan, L., Venugopal, T., & Jayaprakash, M. (2008). Evaluation of the seasonal variation on the geochemical parameters and quality assessment of the groundwater in the proximity of River.

[6]   Reghunath, R., Murthy, T. R. S., & Raghavan, B. R. (2002). The utility of multivariate statistical techniques in hydrogeochemical studies: An example from Karnataka, India. *Water Research, 36*, 2437–2442.

[7]   Belkhiri, L., Boudoukha, A., Mouni, L., & Baouz, T. (2010). Application of multivariate statistical methods and inverse geochemical modeling for characterization of groundwater: A case study of Ain Azel plain (Algeria). *Geoderma, 159*, 390–398.

[8]   Singh, C. K., Kumar, A., Shashtri, S., Kumar, A., Kumar, P., & Mallick, J. (2017). Multivariate statistical analysis and geochemical modeling for geochemical assessment of groundwater of Delhi, India. *Journal of Geochemical Exploration, 175*, 59–71.

[9]   Yidana, S. M., & Yidana, A. (2010). Assessing water quality using water quality index and multivariate analysis. *Environmental Earth Sciences, 59*, 1461–1473.

[10]   Singh, C. K., Kumari, R., Singh, R. P., Shashtri, S., Kamal, V., & Mukherjee, S. (2011). Geochemical modeling of high fluoride concentration in groundwater of Pokhran area of Rajasthan, India. *Bulletin of Environmental Contamination and Toxicology, 86*, 152–158.

[11]   Machiwal, D., & Jha, M. K. (2015). Identifying sources of groundwater contamination in a hard-rock aquifer system using multivariate statistical analyses and GIS-based geostatistical modeling techniques. *Journal of Hydrology, 4*, 80–110.

[12]   Singh, C. K., Shashtri, S., Kumari, R., & Mukherjee, S. (2012). Chemometric analysis to infer hydro-geochemical processes in a semi-arid region of India. *Arabian Journal of Geosciences*, 1–18.

[13]   Yidana, S. M., Ophori, D., & Yakubo, B. B. (2008). Hydrochemical evaluation of the Voltaian system—The Afram Plains area, Ghana. *Journal of Environmental Management, 88*, 697–707.

[14]   Belkhiri, L., & Narany, T. S. (2015). Using multivariate statistical analysis, geostatistical techniques, and structural equation modeling to identify spatial variability of groundwater quality. *Water Resources Management, 29*, 2073–2089.

[15]   Zakariah, M. N. A., Roslan, N., Sulaiman, N., Lee, S. C. H., Hamzah, U., & Noh, K. A. M.; Lestari, W. (2021). Gravity analysis for subsurface characterization and depth estimation of Muda River Basin, Kedah, Peninsular Malaysia. *Applied Sciences, 11*, 6363. https://doi.org/10.3390/app11146363

[16]   Adiat, K. A. N., Nawawi, M. N. M., & Abdullah, K. (2012). Assessing the accuracy of GIS-based elementary multi-criteria decision analysis as a spatial prediction tool: A case of predicting potential zones of sustainable groundwater resources. *Journal of Hydrology, 440–441*, 75–89. https://doi.org/10.1016/j.jhydrol.2012.03.028

[17]   Jamil, H. H., Hassan, W. F. W., & Tan, M. M. (2004). Pengaruh jenis batuan sekitar terhadap taburan Pb dalam sedimen muara Sungai Merbok, Kedah. *Bulletin of the Geological Society of Malaysia, 48*, 7–11.

[18]   Burton, C. K. (1967). The Mahang formation: A mid-Paleozoic euxinic facies from Malaya, with notes on its conditions of deposition and palaeogeography. *Geologie en Mijnbouw, 46*, 167–187.

[19]   Harun, Z., Jasin, B., Mohsin, N., & Azami. (2009). A thrust in the Semanggol formation, Kuala Ketil, Kedah. *Bulletin of the Geological Society of Malaysia, 55*, 61–66.

[20]   Foo, K. Y. (1990). Geology and mineral resources of the Taiping-Kuala Kangsar area, Perak Darul Ridzuan. Geological Survey Headquarters.

[21]   Sajid, Z., Ismail, M. S., Zakariah, M. N. A., Tsegab, H., Vintaned, J. A. G., Hanif, T., & Ahmed, N. (2020). Impact of paleosalinity, paleoredox, paleoproductivity/preservation on the organic matter enrichment in black shales from Triassic turbidites of Semanggol basin, Peninsular Malaysia. *Minerals, 10*, 915.

[22]   Lee, C. P., Leman, M. S., Hassan, K., Nasib, B. M., & Karim, R. (2004). *Stratigraphic Lexicon of Malaysia*. Geological Society of Malaysia.

[23]   Koike, T. (1982). Triassic conodonts from Kedah and Pahang, Malaysia. *Geological Palaeontological Southeast Asia, 12*, 91–113.

[24]   Metcalfe, I. (1981). Permian and early Triassic conodonts from northwest Peninsular Malaysia. *Bulletin of the Geological Society of Malaysia, 14*, 119–126.

[25]   Koike, T. (1982). Triassic conodont biostratigraphy in Kedah, West Malaysia. *Geological Palaeontological Southeast Asia, 23*, 9–51.

[26]   Metcalfe, I. (1990). Lower and middle Triassic conodonts from the Jerus Limestone, Pahang, Peninsular Malaysia. *Journal of Southeast Asian Earth Sciences, 4*, 141–146.

[27]   Metcalfe, I. (1992). Upper Triassic conodonts from the Kodiang Limestone, Kedah, Peninsular Malaysia. *Journal of Southeast Asian Earth Sciences, 7*, 131–138.

[28]   APHA (American Public Health Association). (1995). *Standard methods for the examination of water and wastewater* (19th ed.). American Public Health Association.

[29]   Edmond, J. M., Palmer, M. R., Measures, C. I., Grant, B., & Stallard, R. F. (1995). The fluvial geochemistry and denudation rate of the Guayana Shield in Venezuela, Colombia, and Brazil. *Geochimica et Cosmochimica*

Acta, 59, 3301–3325.

[30] Huh, Y., Tsoi, M., Zaitsev, A., & Edmond, J. M. (1998). The fluvial geochemistry of the rivers of Eastern Siberia: I. Tributaries of the Lena River draining the sedimentary platform of the Siberian Craton. *Geochimica et Cosmochimica Acta, 62*, 1657–1676.

[31] Kumar, A., & Singh, C. K. (2015). Characterisation of hydrogeochemical processes and fluoride enrichment in groundwater of south-western Punjab. *Water Quality Exposure Health*, 1–15.

[32] Cattell, R. B., & Jaspers, J. (1967). A general plasmode (no. 30-10-5-2) for factor analytic exercises and research. *Multivariate Behavioral Research Monographs, 67*, 1–212.

[33] Mondal, N. C., Singh, V. P., Singh, V. S., & Saxena, V. K. (2010). Determining the interaction between groundwater and saline water through groundwater major ions chemistry. *Journal of Hydrology, 388*, 100–111.

[34] Rina, K., Datta, P. S., Singh, C. K., & Mukherjee, S. (2012). Characterisation and evaluation of processes governing the groundwater quality in parts of the Sabarmati basin, Gujarat using hydrochemistry integrated with GIS. *Hydrological Processes, 26*, 1538–1551.

[35] Yakubo, B. B., Yidana, S. M., & Nti, E. (2009). Hydrochemical analysis of groundwater using multivariate statistical methods: The Volta region, Ghana. *KSCE Journal of Civil Engineering, 13*, 55–63.

[36] Alaya, M. B., Saidi, S., Zemni, T., & Zargouni, F. (2013). Suitability assessment of deep groundwater for drinking and irrigation use in the Djeffara aquifers (Northern Gabes, south-eastern Tunisia). *Environmental Earth Sciences, 71*, 3387–3421.

[37] Meybeck, M. (1987). Global chemical weathering of surficial rocks estimated from river dissolved loads. *American Journal of Science, 287*(5), 401–428. https://doi.org/10.2475/ajs.287.5.401

[38] Shanyengana, E. S., Seely, M. K., & Sanderson, R. D. (2004). Major-ion chemistry and groundwater salinisation in ephemeral floodplains in some arid regions of Namibia. *Journal of Arid Environments, 57*, 211–223.

[39] Narany, T. S., Aris, A. Z., Sefie, A., & Keesstra, S. (2017). Detecting and predicting the impact of land use changes on groundwater quality: A case study in Northern Kelantan, Malaysia. *Science of the Total Environment, 599*, 844–853.